

Frequency-Domain On-Off Accumulative Transmission over Frequency-Selective Fading Channels

Jingxian Wu*, Gang Wang*, and Geoffrey Ye Li†

* Department of Electrical Engineering, University of Arkansas, Fayetteville, AR 72701, USA.

† School of Electrical and Computer Engineering, Georgia Institute of Technology, Atlanta, GA 30332, USA.

Abstract— In this paper, we propose a new cross-layer technique that utilizes frequency-domain on-off accumulative transmission (OOAT) in the physical layer to achieve collision-tolerance in the media access control (MAC) layer. The frequency-domain OOAT is developed for wideband systems operating in frequency-selective fading channels. The available spectrum is divided into a large number of orthogonal non-overlapping sub-channels. To achieve collision tolerance, each symbol is transmitted over a set of randomly chosen sub-channels to reduce the probability of collision. Spreading the signal over the frequency-domain also enables frequency diversity, and further improves system performance. Performance of the proposed scheme is analyzed and a performance bound, matched filter bound, is derived. Simulation results show that the proposed scheme can support more active users simultaneously than sub-channels, and it achieves a higher spectral efficiency compared to conventional MAC schemes.

I. INTRODUCTION

In wireless communication networks, cross-layer design and multi-user detection (MUD) are two crucial techniques to ensure the quality of service (QoS) in high information rate transmission, which are limited by the shared medium and the fading of wireless channels [1].

Existing MUD techniques are often used with multi-dimensional signals in the physical (PHY) layer, such as code-division multiple access (CDMA) [2], orthogonal frequency division multiplexing (OFDM) [4], and time-hopping ultra-wide band (TH-UWB) [3] systems, all require that simultaneous users are fewer than the degree-of-freedom of the physical signal, *e.g.* the spreading gain of CDMA or the number of sub-channels in OFDM. Cross-layer design can be performed to combine MUD in the PHY layer with medium access control (MAC) techniques to improve the spectrum efficiency in wireless networks [5]–[10]. One of the most popular joint PHY/MAC layer designs is multipacket reception (MPR) [7]–[10], where a group of packets colliding in the MAC layer can be detected with MUD in the PHY layer. However, most current MPR techniques do not consider practical channel limitations, such as frequency-selective fading, which limit their application in wideband communications.

In this paper, we propose a new frequency-domain on-off accumulative transmission (OOAT) scheme that achieves collision-tolerant MAC with MUD in the PHY layer. The proposed scheme is extended from a time-domain OOAT scheme

in our previous work [11], which can only operate in frequency-flat fading. In the frequency-domain OOAT, the channel is divided into multiple orthogonal sub-channels with the help of OFDM. Different from conventional OFDM, each symbol is transmitted over multiple sub-channels in our scheme. Consequently, the proposed scheme can not only deal with frequency-selectivity of wideband wireless channels as OFDM, but also exploit frequency diversity since each symbol is spread to several sub-channels.

The frequency-domain OOAT scheme converts the relative transmission delays among the users in the time domain into phase shifts in the frequency domain, such that the sub-channels from different users are perfectly aligned. This allows us to carefully plan the on-off patterns employed by different users to minimize the number of users colliding on each sub-channel. Based on the OOAT signal structure, optimum and sub-optimum MUDs are proposed, and an analytical matched filter bound is derived to quantify the performance of the proposed scheme.

II. FREQUENCY-DOMAIN OOAT

A. System Structure

Consider a wireless network with N spatially distributed users transmitting to the same base station (BS) through a one-hop transmission. To achieve collision tolerance in the MAC layer, users employ the frequency-domain OOAT scheme in the PHY layer as shown in Fig. 1. The data from wireless users are divided into frames with K symbols in each frame. The entire available bandwidth, B , is divided into KM sub-channels, with a bandwidth $B_0 = \frac{B}{KM}$ each. Each symbol uses M sub-channels uniformly spread over the entire frequency band. If sub-channels are indexed as $0, 1, 2, \dots, KM - 1$, then the M sub-channels with indices, $\{mK + k\}_{m=0}^{M-1}$, are used for the transmission of the k -th symbol in the slot, for $k = 0, \dots, K - 1$. During each transmission, only R randomly-chosen sub-channels from the M ones are occupied. The indicator vector of the occupied sub-channels for the n -th user can be represented by a binary vector of length M , $\mathbf{p}_n = [p_n(0), \dots, p_n(M-1)]^T \in \mathcal{B}^{M \times 1}$, where $\mathcal{B} = \{0, 1\}$, with $p_n(m) = 1$ if the k -th symbol is transmitted at the $\{mK + k\}$ -th sub-channel, and $p_n(m) = 0$ otherwise. Please note that all symbols from the n -th user use the same transmission pattern \mathbf{p}_n . With such a scheme, each symbol is repeated over R sub-channels (accumulative transmission), and the on-off pattern of the sub-channels are determined by a binary vector \mathbf{p}_n (on-off

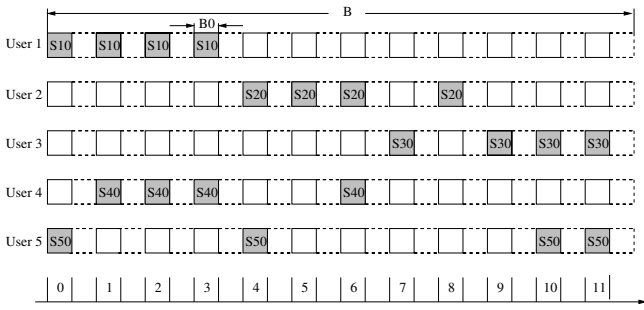


Fig. 1. A frequency-domain OOAT system with $N = 5$ users, $R = 4$ sub-channels occupied out of $M = 12$ sub-channels for each symbol.

transmission). In the example shown in Fig. 1, there are $N = 5$ users, $M = 12$ available sub-channels per symbol, and $R = 4$ out of the 12 available sub-channels are occupied.

Based on the above description, the signal transmitted on the m -th sub-channel of the n -th user can be represented as

$$d_n(m) = p_n(i_m) s_{nk_m}, \quad (1)$$

where $i_m = \lfloor \frac{m}{K} \rfloor$ with $\lfloor a \rfloor$ being the largest integer smaller than or equal to a , s_{nk} is the k -th symbol from user n , and $k_m = [m]_K$ with $[m]_K = m - i_m K$ being the modulo K operator. Consequently, the signal vector of the n -th user for OOAT can be expressed as

$$\mathbf{d}_n = [d_n(0), d_n(1), \dots, d_n(KM - 1)]^T \in \mathcal{S}_+^{L \times 1}, \quad (2)$$

where $L = KM$ and $\mathcal{S}_+ = \{\mathcal{S}, 0\}$, and \mathcal{S} is the modulation constellation set with a cardinality $S = |\mathcal{S}|$.

The signal vector, \mathbf{d}_n , is converted to the time-domain by applying an L -point inverse discrete Fourier transform (IDFT) as

$$\mathbf{x}_n = \mathbf{F} \cdot \mathbf{d}_n, \quad (3)$$

where $\mathbf{x}_n = [x_n(0), x_n(1), \dots, x_n(L-1)]^T$ is the time-domain signal vector, and $\mathbf{F} \in \mathcal{C}^{L \times L}$ is the L -point IDFT matrix with the (r, c) -th element being

$$[\mathbf{F}]_{r,c} = \frac{1}{\sqrt{L}} \exp \left[j2\pi \frac{r \cdot c}{L} \right], \quad r, c = 0, 1, \dots, L-1.$$

Before transmission, a length- μ cyclic prefix (CP) is added to the time-domain signal \mathbf{x}_n to avoid interference between consecutively transmitted frames. The value of μ is chosen as $\mu \geq l_c + l_d - 1$, where l_c is the length of the equivalent discrete-time channel, and l_d is the maximum relative transmission delay among the users. The users are assumed to be quasi-synchronous with $l_d \in [0, M)$.

The time-domain signal vectors from the N users are transmitted to the BS through channels with the frequency-selective fading, and the equivalent discrete-time signal at the BS can be represented by

$$y(i) = \sum_{n=1}^N \sum_{l=0}^{l_c-1} \sqrt{\frac{E_s}{R}} h_n(l) x_n[i-l-l_n]_L + z(i), \quad (4)$$

where E_s is the energy per symbol, $y(i)$ and $z(i)$ are the received sample and additive white Gaussian noise (AWGN) at the i -th sample instant, respectively, l_n is the relative

transmission delay of the n -th user, $h_n(l)$ is the equivalent discrete-time channel impulse response (CIR) between the user n and the BS. The discrete-time CIR includes the effects of the transmit filter, the receive filter, and the physical wireless channel. Due to the time span of the transmit and receive filters, the CIR coefficients, $h_n(l)$, for $l = 0, 1, \dots, l_c - 1$, are correlated, even though the underlying channel might undergo uncorrelated scattering. The correlation coefficient, $c(l_1, l_2) = \mathbb{E} [h_n(l_1) h_n^*(l_2)]$, can be calculated as [12, eqn. (17)].

$$c(l_1, l_2) = \int_{-\infty}^{+\infty} R_{P_T P_R}(l_1 T_s - \tau) R_{P_T P_R}(l_2 T_s - \tau) G(\tau) d\tau, \quad (5)$$

where T_s is the sampling period in the receiver, $G(\tau)$ is the power delay profile of the physical channel, and $R_{P_T P_R}(t)$ is the convolution of the transmit and receive filters.

After the removal of the CP, the received symbols can be written in a matrix form as

$$\mathbf{y} = \sqrt{\frac{E_s}{R}} \sum_{n=1}^N \mathbf{H}_n \cdot \mathbf{x}_n + \mathbf{z}, \quad (6)$$

where $\mathbf{H}_n \in \mathcal{C}^{L \times L}$ is a circulant channel matrix with the first column being $\mathbf{h}_n = [\mathbf{0}_{l_n}^T, h_n(0), h_n(1), \dots, h_n(l_c - 1), \mathbf{0}_{L-l_n-l_c}^T]^T$, and $\mathbf{0}_a$ is a length- a all-zero vector.

The discrete Fourier transform (DFT) is applied to the vector \mathbf{y} to convert the signal to the frequency domain as

$$\mathbf{y}_F = \sqrt{\frac{E_s}{R}} \sum_{n=1}^N \mathbf{G}_n \cdot \mathbf{d}_n + \mathbf{z}_F, \quad (7)$$

where $\mathbf{y}_F = \mathbf{F}^H \mathbf{y}$ and $\mathbf{z}_F = \mathbf{F}^H \mathbf{z}$ are the frequency-domain signal vector and AWGN vector, respectively, and $\mathbf{G}_n = \mathbf{F}^H \mathbf{H}_n \mathbf{F}$ is the frequency-domain channel matrix.

Since \mathbf{H}_n is circulant, \mathbf{G}_n is a diagonal matrix with the m -th diagonal element being

$$G_n(m) = \frac{\exp \left[-j2\pi \frac{l_n \cdot m}{L} \right]}{L} \sum_{l=0}^{l_c-1} h_n(l) \exp \left[-j2\pi \frac{l \cdot m}{L} \right]. \quad (8)$$

Even though the signals transmitted by the different users are quasi-synchronous in the time domain, *i.e.*, they might be mis-aligned for up to M samples, the OFDM symbols from different users are perfectly aligned in the frequency domain as shown in (8) and Fig. 1. The relative delay, l_n , in the time domain is converted to a phase shift, $\exp \left[-j2\pi \frac{l_n \cdot m}{L} \right]$, in the frequency domain.

B. Collision Tolerance

With the frequency-domain system representation in (7), the received information at the m -th sub-channel at the BS is the superposition of the signals, $d_n(m)$. The value of $d_n(m)$ is 0 if $p_n(i_m) = 0$. Therefore, only a subset of the users will collide at the m -th sub-channel. Define the collision order at the m -th sub-channel as $N_c(m) = \sum_{n=1}^N p_n(i_m)$. The collision order of the network is then defined as $N_c = \max_m N_c(m)$. We have $N_c = 2$ for the system shown in Fig. 1.

The frequency-domain OOAT system can be equivalently represented as an N_c -input R -output system similar to the time-domain OOAT system [11]. In practice, to ensure collision tolerance and system performance, it is desirable to have a system with $N_c \leq R$. Due to the perfect alignment of the users in the frequency domain, we can carefully choose the on-off patterns from the different users such that N_c is minimized given N , M and R , which can be performed by exhaustively searching over the set of all the $\binom{M}{R}$ possible patterns.

The frequency-domain OOAT scheme contributes to the performance improvement of the wireless network from the following perspectives. First, the on-off transmission across the sub-channels will reduce the collision order. Second, the transmission of R identical sub-symbols results in a R -dimensional received signal in the frequency domain, which can be used for the detection of the N_c -dimensional signal in the space domain. Third, frequency diversity is achieved by transmitting the k -th symbol in R sub-channels with a fading coefficients of $\{G_n(mK + k)\}_{m=0}^{M-1}$. Fourth, the OOAT signals from different users are perfectly aligned in the frequency domain even if they are not synchronous in the time domain, and this enables the precise control of the collision order by carefully selecting the transmission patterns for all the users.

III. OPTIMUM AND SUB-OPTIMUM DETECTIONS

Here we will discuss the detection of the frequency-domain OOAT signals and develop an optimal and a sub-optimal approach.

A. Optimum Detection

Since all the OFDM symbols are perfectly aligned in the frequency domain as shown in Fig. 1, the k -th symbol from one user will only interfere the k -th symbol from the other users. This is different from the time-domain OOAT [11], where the k -th symbol from one user might interfere the $(k-1)$ -th, k -th, and the $(k+1)$ -th symbols from the other users due to the signal mis-alignment in the time domain.

The perfect alignment among the symbols from all the users in the frequency-domain OOAT determines the k -th symbols from all the N users, $\{s_{nk}\}_{n=1}^N$, can be jointly detected by using a block of M received signal samples $\mathbf{y}_k = [\mathbf{y}_F(k), \dots, \mathbf{y}_F((M-1)K + k)]^T \in \mathcal{C}^{M \times 1}$. The signal vector \mathbf{y}_k can be represented as

$$\mathbf{y}_k = \sqrt{\frac{E_s}{R}} \mathbf{G}_k \cdot \mathbf{s}_k + \mathbf{z}_k, \quad (9)$$

where $\mathbf{s}_k = [s_{1k}, s_{2k}, \dots, s_{Nk}]^T \in \mathcal{S}^{N \times 1}$, and $\mathbf{z}_k = [\mathbf{z}_F(k), \dots, \mathbf{z}_F((M-1)K + k)]^T \in \mathcal{C}^{M \times 1}$ are the modulation symbol vector and noise vector, respectively, and $\mathbf{G}_k \in \mathcal{C}^{M \times N}$ is the frequency-domain channel matrix with the $(m+1, n)$ -th element being $p_n(i_m)G_n(i_m)$.

From (9), the optimum maximum likelihood detector is

$$\hat{\mathbf{s}}_k = \underset{\mathbf{s}_k \in \mathcal{S}^N}{\operatorname{argmin}} \left\| \mathbf{y}_k - \sqrt{\frac{E_s}{R}} \mathbf{G}_k \mathbf{s}_k \right\|^2, \quad (10)$$

where $\|\mathbf{a}\| = \sqrt{\mathbf{a}^H \mathbf{a}}$ is the L_2 -norm of the column vector \mathbf{a} .

The optimum detector in (10) requires the exhaustive search of a set of $|\mathcal{S}|^N$ possible signal vectors. The complexity of the optimum detector grows exponentially with the increase of the modulation level $|\mathcal{S}|$ and the number of users N .

B. Suboptimum Detection

A low complexity sub-optimum detection algorithm is presented in this subsection to balance the trade-off between the performance and complexity. The sub-optimum algorithm is developed by employing an iterative soft-input soft-output (SISO) equalizer, which performs soft successful interference cancellation (SSIC) among the N symbols in \mathbf{s}_k . In this paper, the SISO block decision feedback equalizer (BDFE) [13] is used as the SISO equalizer.

The soft-input to the SISO equalizer is the *a priori* probability of the symbols, $P(s_{nk} = S_i)$, for $n = 1, \dots, N$ and $i = 1, \dots, |\mathcal{S}|$, where $S_i \in \mathcal{S}$. The *a priori* information is obtained from the previous detection round with an iterative detection method, and details will be given later in this subsection. The soft-output of the equalizer is the *a posteriori* probability of the symbols, $P(s_{nk} = S_i | \mathbf{y}_k)$, for $n = 1, \dots, N$ and $i = 1, \dots, |\mathcal{S}|$. With the soft-output at the equalizer, define the *a posteriori* mean, \hat{s}_{nk} , and the extrinsic information, $\beta_{nk}(i)$, of the symbol $s_n(k)$ as

$$\hat{s}_{nk} = \sum_{i=1}^S P(s_{nk} = S_i | \mathbf{y}_k) S_i \quad (11a)$$

$$\beta_{nk}(i) = \log P(s_{nk} = S_i | \mathbf{y}_k) - \log P(s_{nk} = S_i). \quad (11b)$$

The *a posteriori* mean, \hat{s}_{nk} , is used as soft decisions for the SSIC during the SISO-BDFE process. Details of the SISO-BDFE detection can be found in [13].

In the proposed sub-optimum detection, the SISO-BDFE with SSIC will be performed iteratively. At the first iteration, the *a priori* probability is initialized to $P(s_{nk} = S_i) = \frac{1}{|\mathcal{S}|}$. The extrinsic information at the output of the v -th iteration will be used as the soft-input of the $(v+1)$ -th iteration as $P(s_{nk} = S_i) = c_{nk} \exp[\beta_{nk}(i)]$, where c_{nk} is a normalization constant to make $\sum_{i=1}^S P(s_{nk} = S_i) = 1$. At the final iteration, hard decisions will be made based on the *a posteriori* probability generated by the SISO-BDFE as

$$\hat{s}_{nk} = \underset{S_i \in \mathcal{S}}{\operatorname{argmax}} P(s_{nk} = S_i | \mathbf{y}_k). \quad (12)$$

Simulation results show that the performance of the iterative detection algorithm usually converges after 4 iterations. The sub-optimum iterative detection algorithm can achieve a performance that is very close to its optimum counterpart, but with a much lower complexity.

C. Performance Analysis

The matched filter bound on the bit-error rate (BER) of the proposed frequency-domain OOAT scheme with binary phase shift keying (BPSK) is developed in this subsection. With the

interference-free assumption, the received signal corresponding to the k -th symbol of the n -th user can be written as

$$\mathbf{y}_{nk} = \sqrt{\frac{E_s}{R}} \mathbf{g}_{nk} \cdot s_{nk} + \mathbf{z}_{nk}, \quad (13)$$

where $\mathbf{y}_{nk} = [y_F(n_1K + k), \dots, y_F(n_RK + k)]^T$, $\mathbf{g}_{nk} = [G_n(n_1K + k), \dots, G_n(n_RK + k)]^T$, and $\mathbf{z}_{nk} = [z_F(n_1K + k), \dots, z_F(n_RK + k)]^T$ are length- R received sample vector, channel coefficient vector, and noise vector corresponding to s_{nk} , respectively, with n_r being the r -th non-zero position in \mathbf{p}_n .

The channel coefficient vector, \mathbf{g}_{nk} , can be represented as

$$\mathbf{g}_{nk} = \mathbf{B}_{nk} \cdot \mathbf{F}^H \cdot \mathbf{h}_n, \quad (14)$$

where \mathbf{h}_n is the first column of the circulant time-domain channel matrix \mathbf{H}_n , and $\mathbf{B}_{nk} \in \mathcal{B}^{R \times L}$ is a binary matrix, with the $(r, n_rK + k + 1)$ -th element being 1, for $r = 1, \dots, R$, and all other elements of \mathbf{B}_{nk} are zero.

The auto-correlation matrix, $\mathbf{R}_{nk} = \mathbb{E}[\mathbf{g}_{nk} \mathbf{g}_{nk}^H]$, can then be calculated as

$$\mathbf{R}_{nk} = \mathbf{B}_{nk} \mathbf{F}^H \mathbf{R}_{hn} \mathbf{F} \mathbf{B}_{nk}^T, \quad (15)$$

where $\mathbf{R}_{hn} = \mathbb{E}(\mathbf{h}_n \mathbf{h}_n^H)$ is the correlation matrix of the time-domain fading vector. \mathbf{R}_{hn} can be written as a block matrix as

$$\mathbf{R}_{hn} = \begin{bmatrix} \mathbf{0}_{l_n \times l_n} & \mathbf{0}_{l_n \times l_c} & \mathbf{0}_{l_n \times l_r} \\ \mathbf{0}_{l_c \times l_n} & \mathbf{R}_h & \mathbf{0}_{l_c \times l_r} \\ \mathbf{0}_{l_r \times l_n} & \mathbf{0}_{l_r \times l_c} & \mathbf{0}_{l_r \times l_r} \end{bmatrix}, \quad (16)$$

where $l_r = L - l_n - l_c$, and the (l_1, l_2) -th element of $\mathbf{R}_h \in \mathcal{C}^{l_c \times l_c}$ is $c(l_1, l_2)$ defined in (5).

The signal-to-noise ratio (SNR) of (13) can be written as $\gamma = \mathbf{g}_{nk}^H \mathbf{g}_{nk} \frac{\gamma_0}{R}$, where $\gamma_0 = \frac{E_s}{\sigma_z^2}$ is the SNR without fading, with σ_z^2 being the noise variance. For systems with BPSK and Rayleigh fading, the error probability for s_{nk} is [14]

$$P_{nk}(E) = \frac{1}{\pi} \int_0^{\frac{\pi}{2}} \prod_{r=1}^R \left[1 + \frac{\lambda_r \gamma_0}{R \sin^2 \theta} \right]^{-1} d\theta, \quad (17)$$

where λ_r is the r -th eigenvalue of \mathbf{R}_{nk} . The average BER can then be calculated as

$$P(E) = \frac{1}{NK} \sum_{n=1}^N \sum_{k=1}^K P_{nk}(E). \quad (18)$$

IV. SIMULATION RESULTS

Simulation results are presented in this section to demonstrate the performance of the frequency-domain OOAT scheme. The simulation parameters are given in Table I.

Fig. 2 shows the performance of the frequency-domain OOAT under various system configurations. There are $M = 12$ sub-channels per symbol and each symbol is transmitted on $R = 4$ sub-channels. The sub-optimum detection is performed with 4 iterations. The frequency-selective fading is generated with the Pedestrian A power delay profile [15]. The results of the time-domain OOAT in quasi-static flat fading channel

TABLE I
SIMULATION PARAMETERS

Bit rate	3.6864 Mbps
Sub-channel number	1024
Sub-channel bandwidth	3.6 KHz
Symbol number in one frame	100
Time duration of prefix	27.127 us
Tx and Rx filter	Root Raised Cosine
Roll-off factor	0.22
Modulation	BPSK
Frequency selective fading	ITU pedestrian channel A

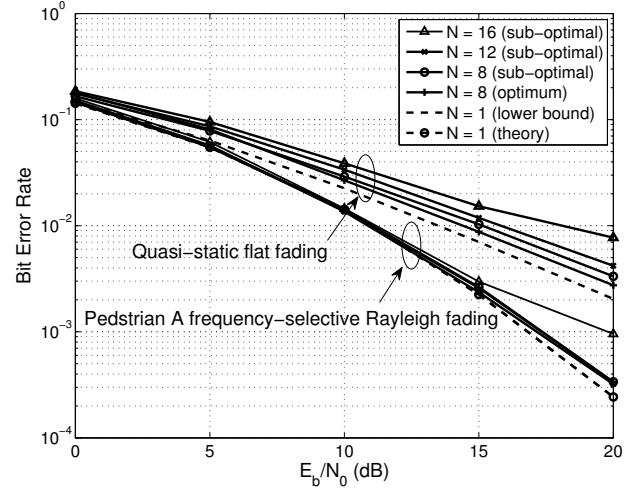


Fig. 2. BER performance of a system with $M = 12$ sub-channels for one symbol, $R = 4$ sub-channels occupied, and various number of users.

are also shown. The frequency-domain OOAT outperforms its time-domain counterpart by 5 dB at $\text{BER} = 2 \times 10^{-3}$ due to the frequency diversity. For the frequency-domain OOAT, the BER performances at $N = 8$ and 12 is almost identical to the collision-free case with $N = 1$, for both the optimum and sub-optimum detections. The matched filter bound overlaps with the $N = 1$ results. When $E_b/N_0 < 15$ dB, the system with $N = 16$ achieves almost the same performance as $N = 1$, and a 3 dB performance degradation is observed for $N = 16$ when $E_b/N_0 > 15$ dB. Therefore, the proposed scheme can support $N > M$ simultaneous users over a large range of practical E_b/N_0 .

Fig. 3 demonstrates the impacts of the number of iterations and the frequency diversity on the frame error rate (FER) performance with $N = 12$. The results labeled with “consecutive transmission” are obtained by transmitting each symbol over M consecutive sub-channels. Uniformly spreading a symbol across the entire bandwidth as in the proposed method will result in a better frequency diversity than transmitting a symbol over M consecutive sub-channels. As expected, the proposed method has a 5.5 dB performance gain over the “consecutive transmission” one at the $\text{FER} = 2 \times 10^{-1}$ thanks to the extra frequency diversity. For both schemes, the biggest performance improvement is achieved at the second iteration. The improvement gradually diminishes as the number of iteration increases, and almost converges at the fourth iteration.

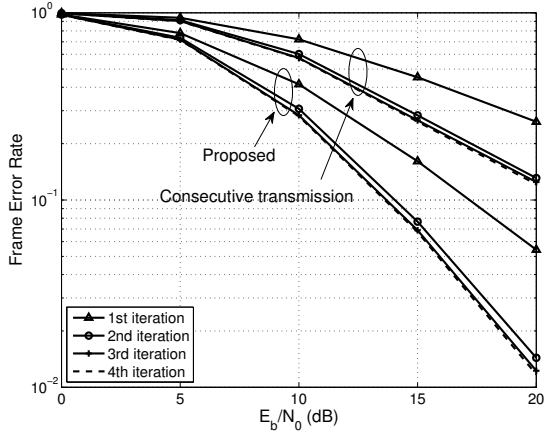


Fig. 3. FER performance of a system with $N = 12$ users, $M = 12$ sub-channels for one symbol, and $R = 4$ sub-channels occupied.

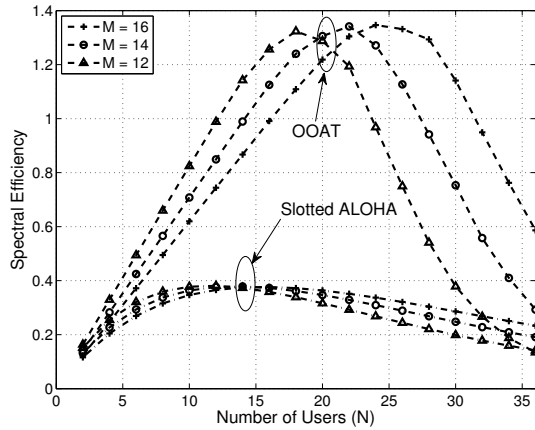


Fig. 4. Spectral efficiency v.s. number of users.

The last example compares the effective spectral efficiency between the frequency-domain OOAT system with the slotted ALOHA system. The spectral efficiency calculation is the same as that in [11]. The E_b/N_0 for both systems is 20 dB. Both systems have the same offered load per user defined by $\frac{1}{M}$ bps/Hz/user. The optimum spectral efficiency of the OOAT system is significantly higher than that of the slotted ALOHA system. For the OOAT system, it is observed that the optimum spectral efficiency can be achieved when $\frac{N}{M} \approx \frac{3}{2}$, e.g., when $M = 16, N = 24$, the maximum spectral efficiency, $\max(\eta_{\text{OOAT}}) = 1.35$ bps/Hz, is achieved. It should be noted that M sub-channels can support $N > M$ users. For the slotted ALOHA system, the optimum spectral efficiency is achieved when $\frac{N}{M} \approx 1$, with a maximum spectral efficiency of $\max(\eta_{\text{ALOHA}}) = 0.38$ bps/Hz. Therefore, under the same offered load per user, the OOAT system can support more users and achieve a spectral efficiency more than three times of that of the slotted ALOHA system.

V. CONCLUSION

A frequency-domain OOAT scheme has been proposed for the cross-layer collision-tolerant MAC operating in frequency-selective fading channels. The collision-tolerance in the MAC layer was achieved by spreading each symbol over multiple orthogonal sub-channels in the frequency-domain in the PHY layer. Optimum and sub-optimum detectors were proposed to jointly recover the information from all the users at the BS, and an analytical matched filter bound was derived based on the structure of the proposed scheme. The frequency-domain OOAT has two improvements over its time-domain counterparts, 1) it can achieve frequency diversity; 2) it has better control of the collision order with all the users perfectly aligned in the frequency domain. The frequency-domain OOAT with M sub-channels achieves the optimum spectral efficiency when there are approximately $N = \frac{3}{2}M$ users.

REFERENCES

- [1] C. Comaniciu, N. B. Mandayam, and V. H. Poor, *Wireless Networks Multiuser Detection in Cross-Layer Design*, Springer, April 2005.
- [2] B. Lu, X. Wang, and J. Zhang, "Throughput of CDMA data networks with multiuser detection, ARQ, and packet combining," *IEEE Trans. Wireless Commun.*, vol. 3, pp. 1576 - 1589, Sept. 2004.
- [3] R. Merz, J. Widmer, J.-Y. Le Boudec, and B. Radunovic, "A joint PHY/MAC architecture for low-radiated power TH-UWB wireless ad hoc networks," *Wireless Commun. Mobile Computing*, vol. 5, pp. 567-580, 2005.
- [4] J. Tao, J. Wu, and Y. Zheng, "Reliability-based turbo detection," *IEEE Trans. Wireless Commun.*, vol. 10, pp. 2352-2361, July 2011.
- [5] P. Casari, M. Levorato, and M. Zorzi, "On the implications of layered space-time multiuser detection on the design of MAC protocols for ad hoc networks," in *Proc. Intern. Symp. Personal, Indoor Mobile Radio Commun. PIMRC'05*, vol. 2, pp. 1354 - 1360, 2005.
- [6] P. Casari, M. Levorato, and M. Zorzi, "MAC/PHY cross-layer design of MIMO ad hoc networks with layered multiuser detection," *IEEE Trans. Wireless Commun.*, vol. 7, pp. 4596 - 4607, Nov. 2008.
- [7] G. Mergen and L. Tong, "Receiver controlled medium access in multihop ad hoc networks with multipacket reception," in *Proc. IEEE Military Commun. Conf. MILCOM 2001*, vol. 2, pp. 1014 - 1018, 2001.
- [8] L. Tong, V. Naware, and P. Venkatasubramaniam, "Signal processing in random access," *IEEE Sig. processing Mag.*, vol. 21, pp. 29-39, Sept. 2004.
- [9] Q. Zhao and L. Tong, "A dynamic queue protocol for multiaccess wireless networks with multipacket reception," *IEEE Transactions on Wireless Communications*, vol. 3, pp. 2221 - 2231, Nov. 2004.
- [10] R. Samano-Robles, M. Ghogho, and D. C. McLernon, "An infinite user model for random access protocols assisted by multipacket reception and retransmission diversity," in *Proc. IEEE Sig. Processing Advances Wireless Commun. SPAWC 2008*, pp. 111 - 115, 2008.
- [11] J. Wu and Y. Li, "Collision-tolerant media access control: on-off accumulative transmission," submitted to *IEEE Trans. Wireless Commun.*, July 2011.
- [12] C. Xiao, J. Wu, S.-Y. Leong, Y. R. Zheng, and K. B. Letaief, "A discrete-time model for triply selective MIMO Rayleigh fading channels," *IEEE Transactions on Wireless Communications*, vol. 3, pp. 1678-1688, Sept. 2004.
- [13] J. Wu and Y. R. Zheng, "Low complexity soft-input soft-output block decision feedback equalization," *IEEE J. Selected Areas Commun.*, vol. 26, pp. 281-289, 2008.
- [14] J. Wu and C. Xiao, "Performance analysis of wireless systems with doubly selective Rayleigh fading," *IEEE Trans. Veh. Technol.*, vol. 56, pp. 721-730, Mar. 2007.
- [15] ITU-R Recommendation M.1225, "Guidelines for evaluation of radio transmission techniques for IMT-2000," 1997.